Martin V. Ferer, National Energy Technology Laboratory (NETL) - U.S. Department of Energy P.O. Box 880, Morgantown, WV 26507-880, U.S.A. and Dept. of Physics, W. Va. Univ., P.O. Box 6315, Morgantown WV 26506-6315, U.S.A
e-mail mferer@wvu.edu;
Phone (304)293-3422 FAX (304)293-5732

Gerhard Kasper, Institut für Mechanische Verfahrenstechnik und Mechanik Universität Karlsruhe (TH), D-76128 Karlsruhe, Germany
e-mail Gerhard.Kasper@MVM.uni-Karlsruhe.de

Achim Dittler,* Institut für Mechanische Verfahrenstechnik und Mechanik Universität Karlsruhe (TH), D-76128 Karlsruhe, Germany
* current address: Dr. Achim Dittler, Daimler Chrysler AG, FTK/A-Knowledge Transfer, HPC G206, D-70546, Stuttgart, Germany
e-mail Achim.Dittler@daimlerchrysler.com

Duane H. Smith, National Energy Technology Laboratory (NETL) - U.S. Dept. of Energy P.O. Box 880, Morgantown, WV 26507-880, U.S.A. and Dept. of Physics, W. Va. Univ,
e-mail DSmith@netl.doe.gov
Phone (304)285-4069; FAX (304)285-4469

# The Transient Regeneration in the Patchy Cleaning of Rigid Gas Filters – Comparison of Modeling to Experiment

Keywords: gas cleaning, rigid filter media, patchy cleaning, modeling, filter regeneration

## 1. Introduction and Objectives

Surface filters are one of the options for particulate removal from gas streams. During the filtration process, filter cake builds up on the surface of the filter medium, and the overall pressure drop of the filter medium increases. To maintain an economical filtration process, the filter cake needs to be removed from the filter media periodically; this is usually accomplished by pulse-jet regeneration. Besides mechanical failure of the filter medium, patchy (incomplete) cleaning [1]-[3] is one of the main problems encountered when regenerating the filter media. Incomplete (patchy) filter regeneration significantly influences the operational performance of the filter media: the lower the regeneration efficiency, the shorter the filter cycle times and the more frequently the filter needs to be regenerated. In extreme cases, the filtration process is not stable and eventually collapses.

Besides dust cake adhesion to the filter surface [4] and operating conditions (e.g. the humidity [5]), the cohesive strength of the dust cake [6] and the structure of the filter medium itself affect the regeneration behaviour of the filter medium. A few studies have modelled the regeneration behaviour for complete filter regeneration on a 2-dimensional microscopic basis [7],[8]. Besides these, other authors report a probabilistic model based on random local filter regeneration [9]. First attempts to compare measured data of the adhesion of a particle layer [10] with results from a physical model which includes local adhesive and cohesive strengths of the dust cake were reported by Ferer [11]. Dittler et al. [12] presented a direct comparison of modeling results with experimental data for transient regeneration phenomena (i.e. the development of regeneration efficiency, local regeneration frequencies, patch size distributions, etc. over a series of filtration cycles ).

Unfortunately, this version of the model did not explicitly include the effects of filter cake compression. In this contribution, we have included filter cake compession in the model. Comparing these modeling results to experiment for incompletely regenerated, rigid filter media. we find much better agreement with experimental results for the filtration pressure. The experiments on transient development of regeneration efficiency, local regeneration frequency and patch size distribution as well as the operational behaviour were performed under ambient conditions in a lab scale filter test rig. In comparing the results of the independent modeling to these data, only four parameters were adjusted. The comparison of the modeling results to experiment provides insight into the reasons for patchy cleaning and shows the influences of cohesive and adhesive bonds as well as of the regeneration parameters on the patchy cleaning patterns, on the local frequency of regeneration, and on the overall regeneration efficiency over a series of filtration cycles. Lastly, the influence of the regeneration behaviour on the operational performance is discussed.

## 2. Project Description and Approach

### 2.1.a Experimental Filter Test Rig

The experimental investigations performed within the scope of the present contribution are carried out in a lab scale filter test rig, which is built according to German VDI guideline 3926 [13]. Figure 1 is a schema of the test rig. It mainly consists of a vertical crude gas channel and a horizontal clean gas extraction tube. The filter coupon (15 cm diameter) under investigation is mounted parallel to the crude gas channel which enables cross flow filtration as experienced in filter housings. Besides the photometric concentration monitor and the control device, an optical measuring system is mounted on the filter test rig opposite the filter coupon. This measuring system, described in detail in [14], enables the full-field in situ measurement of the dust cake height distribution on the surface of the filter medium. From these measurements, we obtain the overall frequency of regeneration as well as the local frequencies of regeneration and the patch size distribution, as discussed later. In addition, we investigate the influence of the regeneration behaviour on the filtration performance (time dependence of filtration cycle times and residual pressure drop) of the filter medium.

### 2.1.b Experimental Determination of Regeneration Efficiency, Local Frequency of Regeneration and Patch Size Distribution

A number of attempts, based on different methods, have been reported for determining the regeneration efficiency of gas cleaning filters. One method determines the regeneration efficiency by measuring the mass of the filter before cleaning and the mass released from the filter medium. This gives a mass-related regeneration efficiency [15]. Another method obtains the regeneration efficiency indirectly from the resistance to flow of the incompletely regenerated filter medium, as given by Cheung [16]. Kanaoka et al. [17] who calculate the regeneration efficiency from the operational data for the pressure drops across a new filter as compared with later cycle data for the pressure drops before and after regeneration. Operational filtration data were compared with fitting equations from a parametric model by Smith, Ahmadi, et al..[18] Regardless of the physical basis on which the regeneration efficiency is obtained, all these methods give an overall regeneration efficiency. Therefore, these methods cannot be used to determine local regeneration efficiencies or local frequencies of regeneration. To measure local frequencies of regeneration, the regeneration of a particular area is determined as follows. A

threshold height value is defined. Regions with dust cake heights below the threshold value are considered to be regenerated, while regions with heights above the threshold value are considered to be un-regenerated. Figure 2 illustrates the procedure schematically. On the left hand side (a) of figure 3 one can see the gray value encoded height profile of the dust cake after the very first regeneration. The very dark grey regions represent dust cake, which was lifted from the surface (adhesive bonds broke) but not removed. The dust cake has been removed from the filter medium in the white regions. On the right hand side, Fig. 3 b), the threshold procedure gives the patchy cleaning pattern, from which we obtain the local frequency of regeneration, the overall regeneration efficiency and the patch size and number. The local frequency of regeneration is obtained by summing up the regeneration efficiencies obtained locally over a number of filtration cycles, whereas the overall regeneration efficiency is simply the ratio of the white area to the total filter area. Patch size and number of patches are a result of image analysis performed with the NIH Image.

### 2.2 Fine-Scale Model of Transient Regeneration

In the physical system which originally motivated this model, a layer of filter cake is deposited on a cylindrical candle filter to some thickness, $t$ ; then a backpulse of compressed air is applied from the inside of the candle filter to blow-off the filter cake, thus cleaning the filter. The force actually responsible for removing the layer of filter cake is due to the pressure drop, P, across the layer. As shown in Figure 4, the model cylinder is cut along a seam and then flattened in the xy plane. Periodic boundary conditions connecting the y=0 and y=L sides preserve the continuity around the cylinder. Of course, the planar filter in the model more closely mimics the present, experimental filter system.

We present a brief overview of our basic model, which has been fully described elsewhere.[19]-[23] In our model, the layer is gridded into rectangular blocks, of base $\ell^2$ and height $T\ell$ , connected to the filter and to each other by spring-like forces. The applied backpulse pressure force, $F = \Delta P\ \ell^2$ , will be balanced by the adhesive and cohesive spring forces (with spring constants $k^a$ and $k^c$, respectively). These spring constants are chosen randomly from particular probability distributions so that the average stiffness of the adhesive springs is 1/2 , and the average stiffness of the cohesive springs is T/2 ( $< k^a > = 1/2$ and $< k^c > = T/2$ ). This thickness parameter, T, gives the ratio of average cohesive to average adhesive strength [19]-[21]. Given the distributions of stiffnesses and the value of the force, F, we perform Gauss-Seidel iterations to determine the displacements. If any adhesive spring is stretched beyond its strength, $S^a$, that spring will break; similarly, if any cohesive spring is stretched beyond its strength, $S^c$, i.e.

$$k^a_{i,j}\varepsilon_{i,j} > S^a_{i,j} \quad \& \quad k^c_{i,j+1} \,|\, \varepsilon_{i,j} - \varepsilon_{i,j+2} \,| > S^c_{i,j+1} \qquad (1)$$

that cohesive spring will break. The strengths are chosen so that the average value of the strength of the adhesive springs is given by $<S^a> = 1/2$ and so that the average value of the strength of the cohesive springs is given by $<S^c> = T/2$ . This model is similar to many models of quasi-static, tensile fracturing in the scientific literature [24]-[26].

In the previous work on this model, the primary focus was the thickness dependence of the backpulse cleaning of a uniformly heterogeneous layer. To study actual operational behaviour, it is essential to characterise the filter-cake redeposition on the patchily cleaned filter surface from one cycle to the next. This adds a number of features affecting the backpulse cleaning, which were not included in the previous modeling:

i) the thickness of the filter cake will no longer be uniform,
ii) uncleaned patches that were raised from the filter surface during cleaning will not re-adhere as strongly to the filter surface during the next filtration cycle,
iii) cracks through the filter cake layer will not completely heal during filtration,
iv) filter cake compression will make uncleaned patches less porous than new patches,
v) there will be a reduction in permeabilities and an increase in the total pressure drop because of filter surface conditioning.

In depositing the filter cake on a patchily regenerated surface, as in point i) above, we assume that the flow velocity through any unit area of the surface is proportional to a permeability for that area. For any unit area

$$\Delta P = K'_1 v + K'_2 W v \qquad (2)$$

where v is the filter face velocity during filtration (e.g. v=5 cm/s) , $K'_1$ is the total specific flow resistance of the filter (e.g. $K'_1$ = 3000 Pa/(m/s) ), $K'_2$ is the specific flow resistance of the filter cake (e.g. $K'_2$ = 120,000 1/s ) and W is the areal mass loading. Being the mass of cake deposited upon a unit area of the filter, the areal mass loading is simply proportional to the thickness t:

$$W = \rho_s ( 1 - \varepsilon ) t \qquad (3)$$

where $\rho_s$ is the density of the solid particles and $\varepsilon$ is uniform porosity. However, for compressible filter cakes the porosity is not uniform. Following Schmidt [27], we subdivide each block of filter-cake into layers, labelled k=1-50, each with their own porosity $\varepsilon_{(i,j)}(k)$, resistance to flow R, mass dW, and strength $\sigma$. As each layer is deposited, the pressure on previously deposited layers is increased; therefore, the porosity of each of previous layers must be increased until the strength of this layer is sufficient to support the increased pressure. After all layers have been deposited the total flow resistance through each block is the sum of the permeabilities due to each layer:

$$K'_2 W_{(i,j)} = r_c \sum_k R(\varepsilon_{(i,j)}(k)) \Delta W_{(i,j)} = r_c R W_{(i,j)} \qquad (4)$$

where $R(\varepsilon_{(i,j)})$ is the flow resistance of a layer with porosity $\varepsilon$ , $\Delta W_{(i,j)}$ is the mass deposited in that layer and $r_c$ contains the porosity and mass independent constants multiplying $RW_{(i,j)}$ to give the permeability of that layer.[27]

In this version of the filter cake removal model, we assume a 'bundle-of-tubes' type flow, where the flow resistance is perpendicular (no cross flow) through any one block (i,j) of area A, so that the flow resistance is given by the flow resistance of that block

$$v_{(i,j)} = ( \Delta P / r_c ) / ( R_f + RW_{(i,j)} ) . \qquad (5)$$

Although it has been shown that horizontal flows can be important, [27] this simple approximation will give an estimate of the real filter-cake height variations occurring as the

filtration/cleaning process is cycled. Furthermore, we assume that the pressure drop is uniform over the surface.

In filtration, the average flow velocity is constant (e.g. $v = 5$cm/s, $v = 5$). We equate our average volume flow velocity $<q_{(i,j)}>$ to the constant volume flow velocity $q_f$ , and therefore the average velocity to the constant velocity, $v_f = 5$,

$$<v_{(i,j)}> = (\Delta P/r_c) < (R_f + RW_{(i,j)})^{-1} > = v_f \quad (6)$$

This determines the filtration pressure drop as a function of time

$$\Delta P(t) = r_c \, v_f / < (R_f + RW_{(i,j)})^{-1} > \quad (7)$$

in terms of the constants, $r_c$, R, and $v_f$ and of the distribution of resistances, $RW_{(i,j)}$ at time t. In turn, Eqs. (5) and (7) can be used to determine the flow velocity through block (i,j) at time t, so that the rate of filter cake deposition on block (i,j) at time t is given by

$$\left(\frac{dW_{(i,j)}(t)}{dt}\right) = \eta \, q_{(i,j)} = \eta \, A v_{(i,j)} = \eta \, A \, (v_f / < (R + RW_{(i,j)})^{-1} >) / (R + RW_{(i,j)}), \quad (8)$$

where A is the cross-sectional area of one block, and where $\eta$ is the mass density of filter cake deposited per unit volume of gas filtered. Integrating Eq. 8 from the time immediately after cleaning, $t_o$ , to the end of the filtration cycle at some final time, $t_f$, one determines the resistance distribution, each $RW_{(i,j)}$, after the filtration cycle

$$RW_{(i,j)}(t_f) = RW_{(i,j)}(t_o) + \int_{t_o}^{t} \frac{R dW_{(i,j)}(t)}{dt} dt = RW_{(i,j)}(t_o) + \int_{t_o}^{t_f} \frac{v_f \eta}{< (R + RW_{(i,j)})^{-1} > (R + RW_{(i,j)})} dt \quad (9)$$

where the final time is to be determined by operating conditions, e.g. i) if the filtration ends at $t_f$ , when the pressure reaches the same maximum value at the end of every cycle, or ii) if the filtration ends at the same $t_f$ for every cycle.

Having determined the thickness distribution after filtration, we assign values of cohesive bonds between any two blocks based upon the block with the minimum thickness. However, the procedure is different, if there is a broken cohesive bond (i.e. if there is a broken cohesive bond between two blocks which were not removed); the cohesive bond is only formed between the additional deposition on these two blocks. The deposition described above provides a simple but hopefully accurate approximation to the actual filter cake deposition. Our results agree with the theoretical predictions of Dittler and Kasper [27],[28]. In feature ii) of the model, it was observed that numerous patches of filter cake are lifted but not removed during backpulse cleaning. It seems reasonable that these patches will not significantly re-adhere during a subsequent filtration cycle because that part of the surface is shielded during new deposition. Therefore, these patches which are lifted but not removed will be more weakly attached, so that they can be more easily removed during the next cycle. This effect has been directly observed in the experiments of Dittler and Kasper [29]. In our model, we assume no re-attachment of those blocks of filter-cake which were lifted but not removed. If the blocks had re-attached with their original strength, the filter-cake would be essentially the same after each filtration cycle, so that essentially the same blocks would be removed during each regeneration, making the frequency of regeneration dramatically different from that observed experimentally. Since many of the properties of interest depend sensitively upon the regeneration efficiency, it is important for any modeling runs to correctly reproduce the regeneration efficiency from one cycle to the next. This takes some care because the experimental efficiency depends upon any number of operating conditions (notably filter-cake compression and conditioning of the filter surface ) which are difficult to

characterise accurately enough to input into a model for predicting the regeneration efficiency.

The consequences filter-surface conditioning (decrease in effective filter permeability and resulting increases in pressures and filtration efficiency) can be incorporated into the model by adjusting the backpulse pressure force.

## 3. Results: Comparison of Modeling and Experimental Results

The basic purpose of this section is to determine what rules for filter-cake deposition in the model will give the best agreement with experiment. We will also determine the best values of the four adjustable parameters used in the model.

### 3.1 Regeneration Behaviour

In attempting to compare the modeling results with experiment, it was necessary to be able to reproduce the cycle-to-cycle regeneration efficiency. This involved a proper choice of backpulse cleaning force. More subtly, it was important to mimic the filter-surface conditioning (points 'iv)' and 'v)' in the earlier discussion), which would most noticeably change the backpulse cleaning force and consequently the filter regeneration for the first few cycles. Filter conditioning reduces the permeability of the filter causing a smaller pressure drop across the filter-cake after the first few cycles; therefore, the actual backpulse cleaning force decreases during the first few cycles**.** In a simple attempt to mimic the conditioning of the filter surface (point 'v)'), we have introduced an 'ad-hoc' reduction in the strength of the backpulse pressure force relative to the average filter cake strengths, as the modeling proceeds from one cleaning cycle to the next. This assumes the same average conditioning over the filter surface. In practice, we kept the average adhesive strength fixed at the value of 1/2 and introduced a rather sharp decrease in the maximum backpulse pressure $0.275\ (1.0 + 1.1/5^{n})$ , for cleaning cycle n. Of course, during each of the n regeneration cycles, the backpulse pressure pulse exerts a cleaning pressure which decreases from the maximum value as the filter cake is removed. This expression for the maximum pressure, the first of the four adjustable parameters, gave good qualitative agreement with experimental regeneration efficiencies from cycle-to-cycle. Without this reduction factor, the modeling would always predict less cleaning in the first cycle than in any subsequent cycle; numerous experiments show more efficient cleaning during the first one or two cycles than during subsequent cycles, which can be understood in terms of the higher permeability of the virgin filter causing a higher removal pressure (pressure drop across the filter cake) during the first few cycles. Figure 5 shows the regeneration efficiency from this modeling, decreasing from approximately 32% in the first cycle to approximately 27% in the last cycles. As illustrated in Fig. 5, this agrees well with experimental results, which typically show such a decrease from the first few cleaning cycles to later cycles. The differences in the first two cycles would have been reduced by a slightly smaller decrease in the maximum backpulse pressure.

### 3.2 Frequency of Regeneration

To achieve agreement with remainder of the experimental results, it was necessary to invoke feature 'iii)', from section 2.1.1. In an earlier version of the modeling, we had assumed that all of the broken cohesive bonds had reformed to their full strength characterised by the new deposition. With this assumption the modeling results were radically different from the experimental results. In the modeling to be discussed, we assumed that for any broken cohesive bond between two blocks, neither of which were removed, only the newly deposited filter cake formed a cohesive bond and that no fraction of

the broken cohesive bond between the previously deposited filter cake was re-formed (healed).

To illustrate these rules, Figure 6 shows a cross-section of the filter and filter-cake (newly deposited filter cake is shaded darker grey). As in the actual model, more new filter cake is deposited on cleaned areas (e.g. the second block) than on the thicker, existing layers (especially the first and last blocks). There was a broken adhesive bond between the filter and the fourth block, and a broken cohesive bond between this fourth block and the fifth block. The model assumes that this adhesive bond (adhesive bonds are shown by a series of vertical lines) was not reformed upon the deposition of new filter cake during filtration. The model assumes that a cohesive bond (series of horizontal lines) is only formed by the new filter cake deposition between the fourth and fifth blocks. The cohesive bonds connecting the second block to its neighbours are weaker because the thickness associated with the bond strength between two blocks is determined by the thinner of the two blocks.

In comparing the frequencies of regeneration from the modeling with those from experiment, it is clear that the agreement, although not perfect, is very good. Fig. 7a gives the Portion of Surface vs. Frequency of Regeneration after ten filter cycles. In the modeling 28% of the blocks are never removed (vs. 26% from experiment); 16% are removed only once (vs. 18% from experiment); etc. until 7.5% are removed 10 times (vs. 5% from experiment). Figure 7b gives the local frequency of regeneration corresponding to figure 7a. The local frequency of regeneration distributions look very similar when one adjusts for the difference in scale: the round filter coupons are 14cm in diameter while the model filter rectangles are 10.27 cm. x 6.4 cm. It is instructive to contrast this version of the model with the early version that healed all broken cohesive bonds. In the early version, 55% of the blocks were never removed; 12% were removed once; 6% were removed twice; and so forth. Because 55% of the blocks remained in place for all ten cycles, the local frequency of regeneration plots had much more white space than the result on the right of Fig. 7b). Therefore the modeling provides results in much better agreement with experiment when the broken cohesive bonds are not restored.

### 3.3. Patch Size

If one i) chooses the value of the adjustable thickness paramter, T=0.5, and ii) scales the modeling system, so that each of the 16000 blocks has an area $A = \ell^2 = 0.4$ mm$^2$ ( the 100x160 block model systems corresponds to a size of 10.27 cm x 6.4 cm), then the modeling results for patch size agree well with experiment. In determining the value of T and the physical size of the blocks, the second and third of the four adjustable parameters are determined. Figs. 8 gives the patch size distribution obtained from the experiment (a) and from our modeling (b). When comparing the patch size distributions, one can see that both, experiment and modeling, show the same tendencies. First, for the chosen thickness, T = 0.5, in the tenth cycle, approximately 39% of the patches have an area less than 1 mm$^2$ (vs. 35% from experiment) and 84% of the patches have an area less than 10 mm$^2$ (vs. 86% from experiment). This agreement is very sensitive to the value of T. For T=0.6, 35% of the patches have an area less than 1 mm$^2$, while only 75% of the patches have an area less than 10 mm$^2$ (in comparison with $\approx$ 85% for experiment and the T=0.5 model). This shows that the larger cohesive forces favor demonstrably larger patches in that 25% of the patches are larger than 10 mm$^2$ for the T=0.6 model vs. $\approx$15% from experiment and the T=0.5 model Second, the patches become smaller for the later regeneration cycles; the opposite tendency (patches became larger) was observed in the early version of the model where the cohesive

bonds were healed. This decrease in patch size can also be seen in figure 9. Fig. 9 displays the median patch size $A_{50}$ vs. cycle number. There is very good agreement of the curves for cycles 4 and higher. For low cycle numbers, the patches obtained from experiment are larger than those given from modeling; this might be due to the conditioning of the filter medium, and might be related to the larger regeneration efficiency (Fig. 5 ) for the first two cycles. For cycles 4 and higher, the median patch from modeling is approximately (5 blocks)x(0.4 $mm^2$/block) = 2 $mm^2$. This is very close to the median size from the experimental distribution (Fig. 8a).

### 3.4. Operating Behaviour

As discussed elsewhere (e.g. [30]), the regeneration behaviour has a major influence on the operational behaviour of the filtration process and hence on the dust cake build-up. The operational behaviour can be characterized by the pressure drop curve and its dependence on the filter cycle number.

#### 3.4.1 Pressure Drop Curves

Figs. 10 gives the pressure drop vs. filtration time for cycles 1,2,5, and 10 obtained from our experiments (a) and from our model (b). The factor, $\eta$, in Eq. (8) is the fourth adjustable parameter; this determines the time scale during filtration. It can be seen from fig. 10b that the pressure drop curves from modeling correctly mimic the shape of the experimental curves. In the model, the pressure drop curves for cycle 2, 5 and 10 have the same convex shape as the experimental curves; the differences in filtration time are most likely due to the small differences in regeneration efficiency. [31]. ***The effect of dust cake compression has a significant influence on the operational performance of the filtration process.*** Comparing Figure 10b with Figure 10a of Dittler et al. in ref. [12], shows the effect of adding filter cake compression to the model.

## 4. Applications and Future Activities

Patchy cleaning is widely observed when gas cleaning filter media are regenerated incompletely. In order to investigate the filter regeneration behaviour and its influence on the operational performance of rigid filter media over a series of filtration cycles, experiments were performed in a filter test rig built in accordance with German VDI guideline 3926. This test rig was equipped with a measuring system capable of measuring the dust cake height on the filter medium surface with a high lateral and topographical resolution. With this measuring system, information about the overall regeneration efficiency, the local frequency of regeneration, and the number and size of regenerated areas was obtained over a multitude of filtration cycles. The modeling results were compared to the experimental results.

The original two-dimensional grid model was developed to study layer removal during the first cycle. [19]-[23] In accounting for adhesive, as well as cohesive properties of the dust cake, this model produced results in good agreement with experiment.[11] In a recent paper, we extended the model to a series of cycles by using a simple rule for depositing incompressible filter cake on a patchily cleaned surface.[12] In this extension of the previous work, we have included the compressibility of the filter cake.[27] The inclusion of compressibility significantly improved the modeling results for filtration pressure (Figs. 10). As discussed in section 3, use of only four adjustable parameters in this version of the model produced results in good agreement with the comprehensive set of experiments.

Achieving this level of agreement with the room-temperature experiments necessitated the assumption that any adhesive or cohesive bond broken during a regeneration cycle was not reformed during subsequent filtration cycles. If the model restored the

adhesive bonds between uncleaned patches of filter cake and the filter, essentially the same patches were removed during each regeneration, which is in striking disagreement with the experimental frequency of regeneration (Fig. 7a). If the model restored the cohesive bonds between uncleaned blocks of filter cake, i) the patch size increased from cycle-to-cycle in disagreement with experiment (Figs. 8a & 9), ii) too many of the same blocks were removed every time in disagreement with the experimental frequency of regeneration (Fig. 7a) and iii) after the first cycle, the filtration pressure decreased from cycle-to-cycle in disagreement with the experimentally observed increase (Fig. 10a). Therefore, the model development was guided by our extensive experimental results. Consequently, the modeling indicates that in these experiments bonds only form between newly deposited particles in the filter cake, and that once these bonds are broken, they do not re-heal. Of course, different filtration parameters (more reactive dust particles and elevated temperatures) may lead to different conclusions. Since we have a predictive model of the filtration process, we intend to investigate these issues.

## References


[1] Koch, D.; Seville, J.P.K.; Clift, R. "Dust-Cake Detachment from Gas Filters" - Powder Technology, 86, 1996, pp. 21 – 29

[2] Duo, W.; Seville, J.P.K.; Kirkby, N.F.; Büchele, H.; Cheung, C.K."Patchy Cleaning of Rigid Gas Filters: II" - Chemical Engineering Science, 52 (1), 1997, pp. 153 – 164

[3] Seville, J.P.K.; Cheung,W.; Clift,R. "Patchy Cleaning Interpretation of Dust Cake Release from non-Woven Fabrics' - Filtration & Separation, May/June 1989, pp. 187 – 190.

[4] Morris, K.; Allen, R.W.K.; Clift, R. "Adhesion of Cakes to Filter Media" - Filtration & Separation, January / February 1987, pp. 41 – 45

[5] Pilz, T.; Löffler, F. "Influence of Humidity upon Dust Separation with Surface Filters" - Preprints Filtec Conference, Karlsruhe, 1995, pp.139 – 148

[6] Pilz, T.; Löffler, F. "Einfluβ adhasiver und kohasiver Partikeleigen-schaften bei der Filtration on Oberflachenfiltern", - Chem.-Ing.-Techn., 67, 1995, pp. 745 – 749

[7] Stöcklmayer, Ch.; Höflinger, W. "Simulation of the Long-Term Behavior of Regenerable Dust Filters"– Filtration & Separation, May 1998, pp. 373 – 377

[8] Stöcklmayer, Ch.; Höflinger, W. "Simulation of the Regeneration of Dust Filters" – Mathematics and Computers in Simulation, 46, 1998, pp. 601 - 609

[9] Duo, W.; Kirkby, N.F.; Seville, J.P.K.; Clift, R. "Patchy Cleaning of Rigid Gas Filters: I" - Chemical Engineering Science, 52 (1), 1997, pp. 141 – 151

[10] Schmidt, E. "Experimental Investigation into the Detachment of Differently Structured Particle Layers from Surfaces"–Chem. Eng. Technol. 21 (1988), pp. 26 – 29

[11] Ferer, M.V.; Smith, D.H. 'Filter Cake Removal Efficiency: Comparison of Modeling Results with Experiment', Chemical Engineering Science, 55 (21), 2000, pp. 5003 - 5011

[12] Dittler, A., et al., 'Patchy Cleaning of Rigid Gas Filters-Transient Regeneration Phenomena: Comparison of Modeling to Experiment ', Powd. Tech., 124, 55-66 (2002).

[13] VDI Richtlinie 3926 - VDI Handbuch Reinhaltung der Luft - Band 6, 1994

[14] Dittler, A.; Gutmann, B.; Lichtenberger, R.; Weber, H.; Kasper, G. - Powder Technology, **99** (2), 1998, pp. 177 – 184

[15] R. Klingel, "Untersuchung der Partikelabscheidungaus Gasen an einem Schlauchfilter mit Druckstoβabreinigung"-VDI-Fortschrittsberichte,Reihe3: Verfahrenstechnik, Nr. 76, 1982

[16] W. Cheung, "Filtration and Cleaning Characteristics of Ceramic Media" - Ph.D. Dissertation, University of Surrey, Guilford, U.K., 1989

[17] C. Kanaoka, T. Kishima, M. Furuuchi "Accumulation and Release of Dust from rigid ceramic filter element" - High Temperature Gas Cleaning (Schmidt, Gäng, Pilz, Dittler: eds.), 1996, pp. 183 – 192
[18] Duane H. Smith, et al. , 'Analysis of Operational Filtration Data' I Powd. Tech. **94** 15 (1997); II Powd. Tech. **97** 139 (1998); and III Aerosol Sci. and Tech. **29** 224 (1998).
[19] Ferer, M.; D. H. Smith, ' A Simple Model of the Adhesive Failure of a Layer - Cohesive Effects', J. Appl. Phys., **81**, 1737-1744, (1997).
[20] Ferer, M.; D. H. Smith, 'Continuous Behavior in a Simple Model of the Adhesive Failure of a Layer ', Phys. Rev. E, **57**, 866-874, (1998).
[21] Ferer, M.; D. H. Smith, ' Modeling of Backpulse Filter Cleaning: The Small Particle Filter Cake Fragments', Aerosol Sci. Technol., **29**, 246-256, (1998).
[22] Ferer, M.; D. H. Smith, ' The Transition from Continuous to Discontinuous Material Failure in a Simple Model of an Adhesive Layer', Phys. Rev. E, **58**, 7071-7078, (1998).
[23] Ferer, M.; D. Smith, 'A Simple Model of Filter Caker Removal', High Temp. Gas Cleaning, Karlsruhe Germany, Sept. 1999, pp. 172-184.
[24] Hermann, H. J.; Roux, S. - "Statistical Models for the Fracture of Disordered Media," 1990 North Holland, Amsterdam.
[25] Meakin, P., Models for Material Failure" - Science, 252, (1991), pp. 226-234.
[26] Duxbury, P. M.; Leath, P.L.; Beale, P.D., "Breakdown Properties of Quenched Random Systems: the Random Fuse Network" - Phys. Rev. B, 36 (1987), pp. 367-380.
[27] Schmidt, E. Theoretical Investigations into the Copmpression of Dust Cakes Deposited on Filter Media, Filtration and Separation, May 1997, pp365-368.
[28] Dittler, A.& G. Kasper, Hi-T. Gas Cleaning, Karlsruhe Germany, Sept. '99, pp.119-127.
[29] Dittler, A.&G. Kasper, Hi-T. Gas Cleaning, Karlsruhe Germany, Sept. '99, pp. 164-171.
[30] Dittler, A.; Kasper, G. - 'Patchy Cleaning of Rigid Filter Media' - World Filtration Congress 8, Brighton, U.K., 3. – 7. April 2000 – Proceedings Vol. I, pp. 333 – 336
[31] A. Dittler, G. Kasper – Presentation at the GVC Fachausschuß „Gasreinigung“,1Würzburg, Germany, 2000.

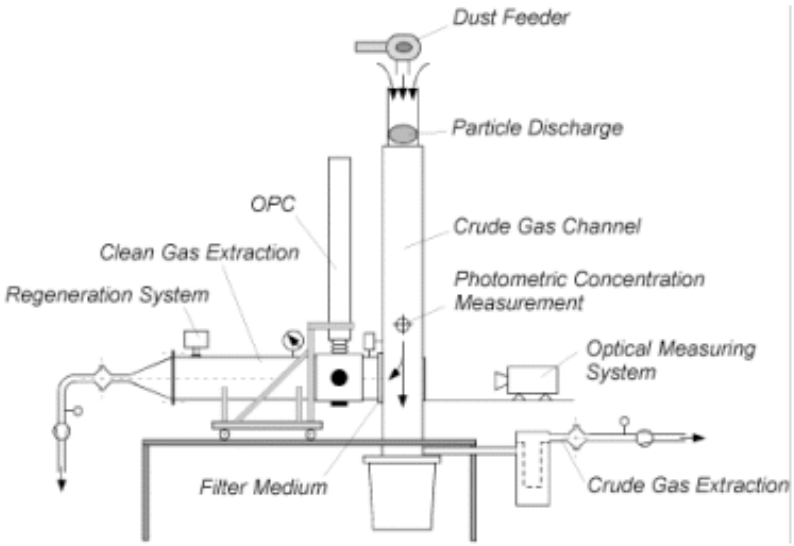


**Figure 1** Lab Scale Filter Test Rig

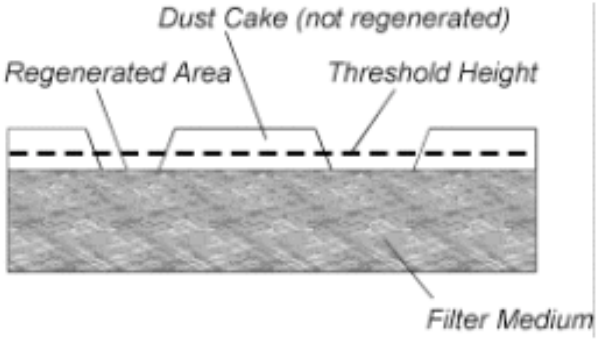


**Figure 2** Schematic of Filter/Filter-Cake cross-section showing the threshold height for determination of local regenerations

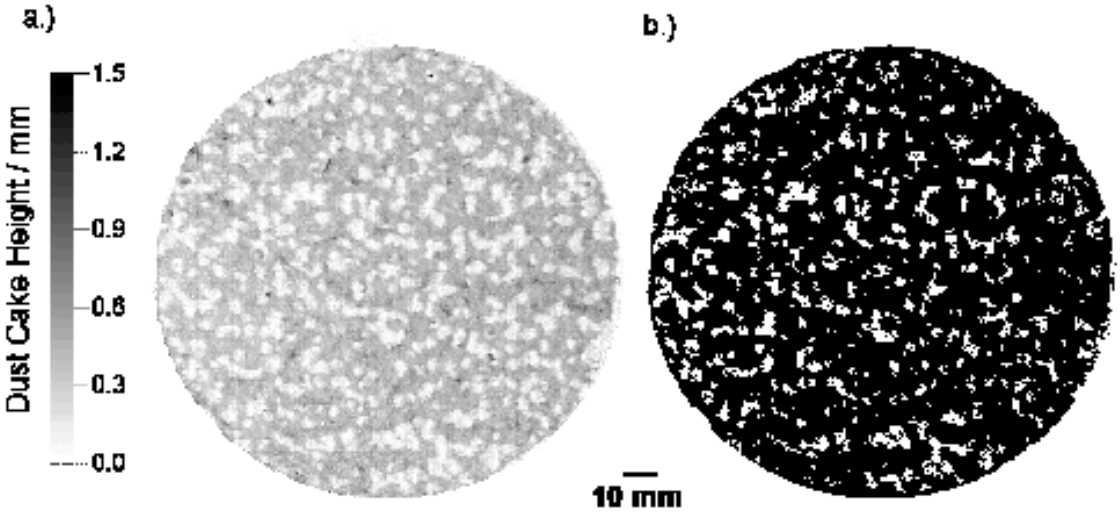


***Figure 3 a)*** This shows the gray-scale encoded height profile; the threshold procedure gives the patchy cleaning pattern shown in **b)** on the left (white patches are cleaned).

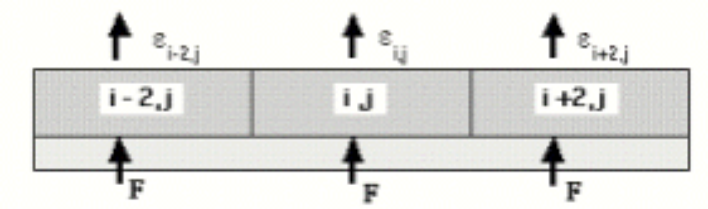


***Figure 4*** The figure shows the imaginary gridding of the filter cake on the surface of the filter.

**Figure 5** compares the regeneration efficiency from modeling to the efficiency from experiment.

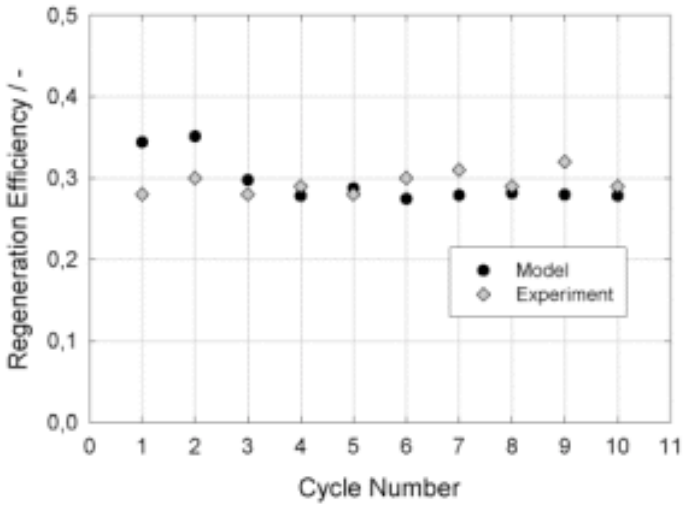


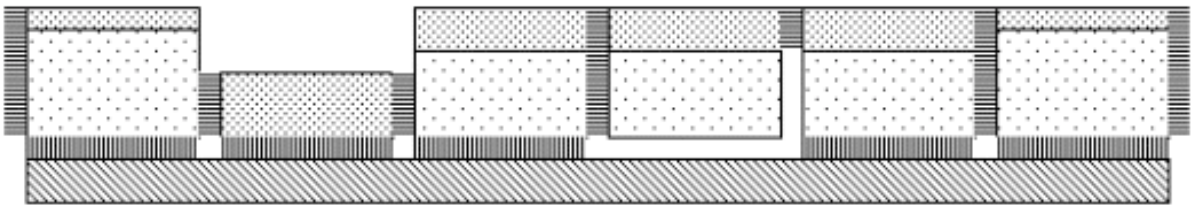

**Figure 6** shows a cross-section of the filter cake after a later filtration cycle. The vertical lines represent adhesive bonds; the horizontal lines represent cohesive bonds; the darker gray shading shows newly deposited filter cake.

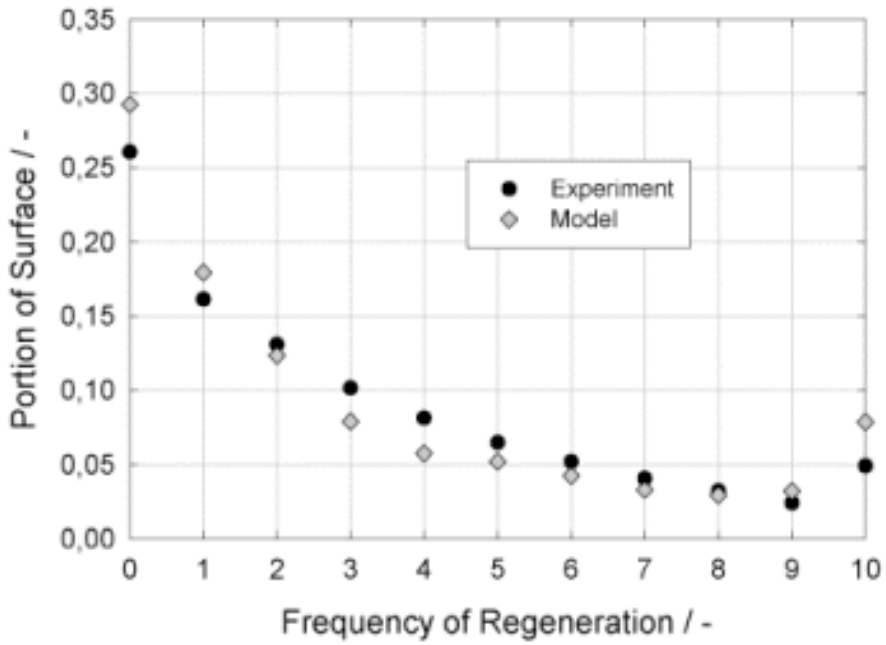


***Figure 7a*** This frequency of regeneration plot shows the fraction of the surface cleaned zero times, once during the ten cycles, twice, and so forth..

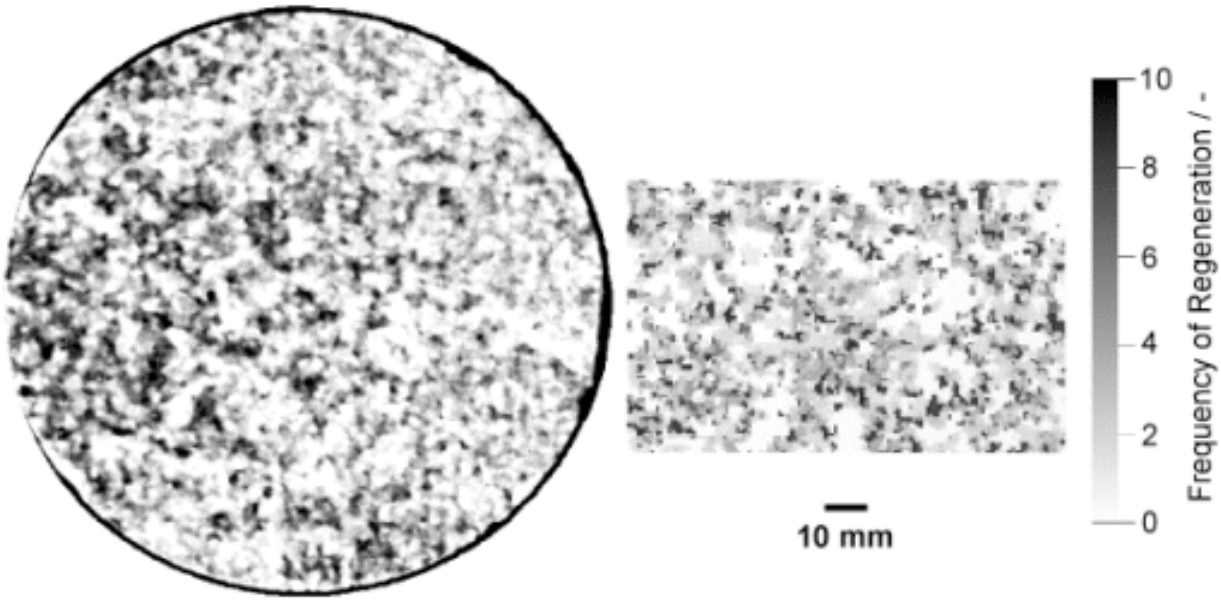


**Figure 7b** shows the local frequency of regeneration . The darkest regions are cleaned all ten cycles; the lightest gray regions are cleaned once. The size of the modelling results , on the right, are scaled to the physical size of the experimental results as discussed in the next section.

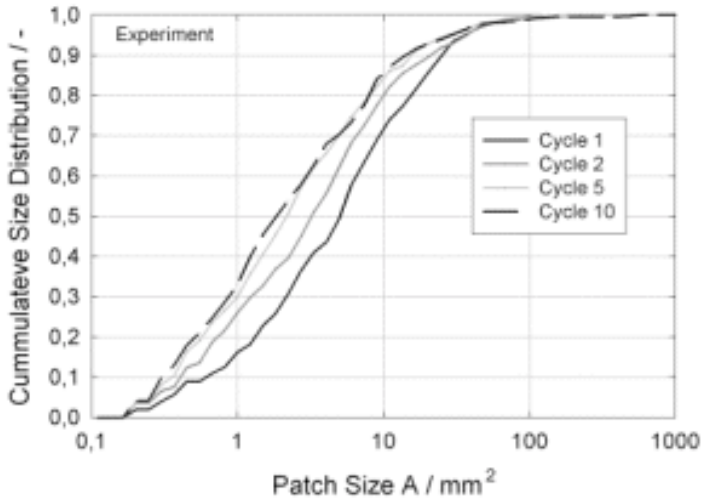


**Figure 8a,** shows the cumulative Patch Size Distribution from Experiment.

***Figure 8b*** *shows the cumulative Patch Size Distribution from Modelling.*

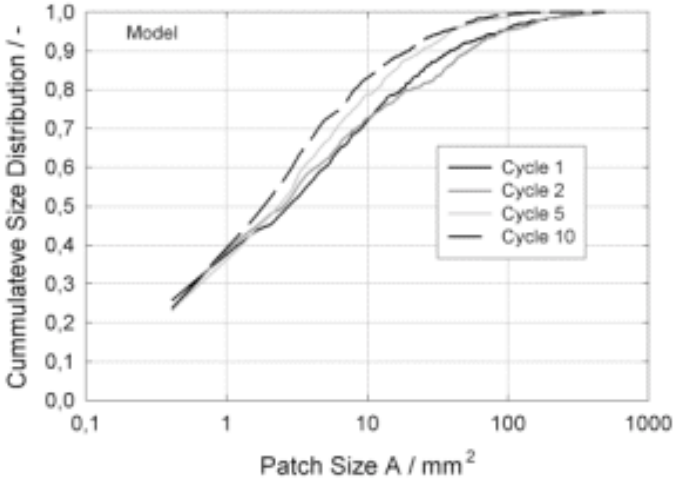


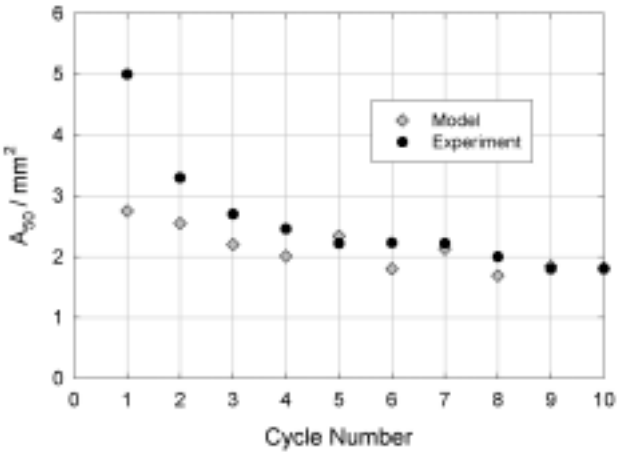


**Figure 9** shows the median size of the cleaned patches from both the experiment and the model.

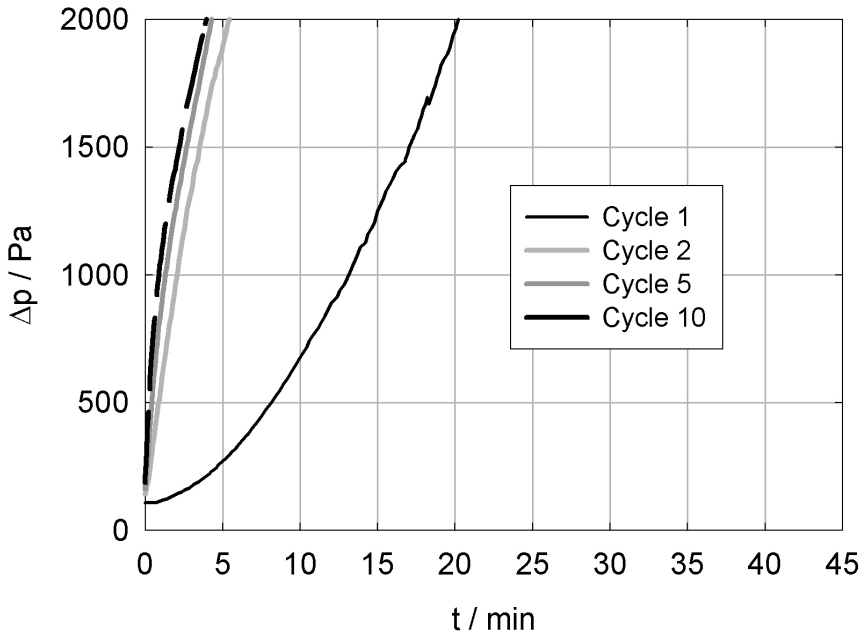


**Figure 10 a** Pressure drop vs. time during filtration cycles #1, #2, #5, and #10 from experiment.

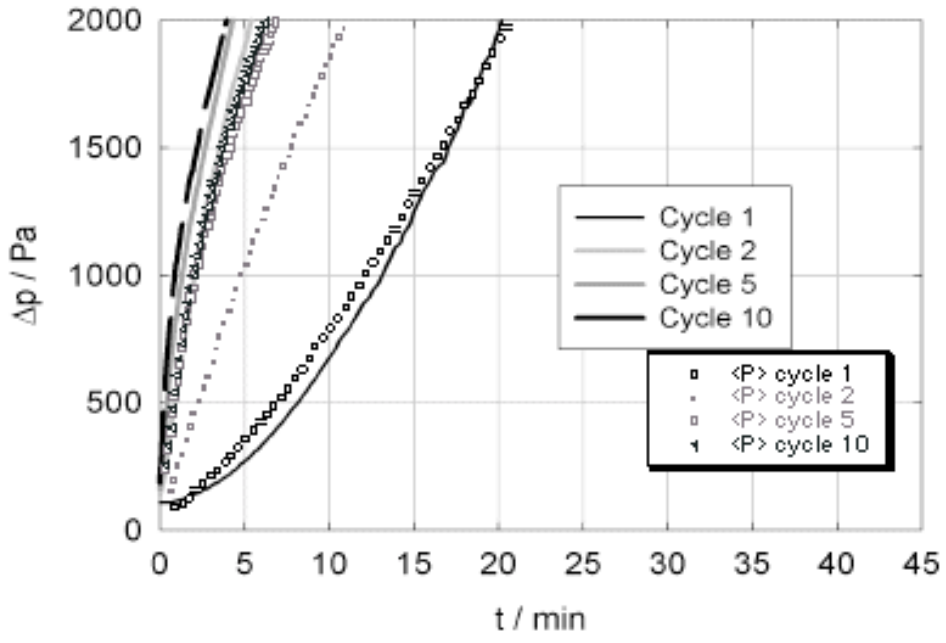


**Figure 10 b** Pressure drop vs. time during filtration cycles #1, #2, #5, and #10, comparing modeling results (open plot symbols) to experiment (lines as in Fig. 10 a).